

9-2008

# Use of Fluorinated Functionality in Enzyme Inhibitor Development: Mechanistic and Analytical Advantages

David B. Berkowitz

*University of Nebraska - Lincoln*, dberkowitz1@unl.edu

Kannan R. Karukurichi

*University of Nebraska - Lincoln*

Roberto de la Salud-Bea

*University of Nebraska - Lincoln*

David L. Nelson

*University of Nebraska - Lincoln*

Christopher D. McCune

*University of Nebraska-Lincoln*, cmccune2@unl.edu

Follow this and additional works at: <http://digitalcommons.unl.edu/chemistryberkowitz>



Part of the [Chemistry Commons](#)

---

Berkowitz, David B.; Karukurichi, Kannan R.; Salud-Bea, Roberto de la; Nelson, David L.; and McCune, Christopher D., "Use of Fluorinated Functionality in Enzyme Inhibitor Development: Mechanistic and Analytical Advantages" (2008). *David Berkowitz Publications*. 10.

<http://digitalcommons.unl.edu/chemistryberkowitz/10>

This Article is brought to you for free and open access by the Published Research - Department of Chemistry at DigitalCommons@University of Nebraska - Lincoln. It has been accepted for inclusion in David Berkowitz Publications by an authorized administrator of DigitalCommons@University of Nebraska - Lincoln.

Published in final edited form as:

*J Fluor Chem.* 2008 September ; 129(9): 731–742. doi:10.1016/j.jfluchem.2008.05.016.

## Use of Fluorinated Functionality in Enzyme Inhibitor Development: Mechanistic and Analytical Advantages

David B. Berkowitz, Kannan R. Karukurichi, Roberto de la Salud-Bea, David L. Nelson, and Christopher D. McCune

Department of Chemistry, University of Nebraska, Lincoln, NE 68588-0304

### Abstract

On the one hand, owing to its electronegativity, relatively small size, and notable leaving group ability from anionic intermediates, fluorine offers unique opportunities for mechanism-based enzyme inhibitor design. On the other, the “bio-orthogonal” and NMR-active  $^{19}\text{F}$ -fluorine nucleus allows the bioorganic chemist to follow the mechanistic fate of fluorinated substrate analogues or inhibitors as they are enzymatically processed. This article takes an overview of the field, highlighting key developments along these lines. It begins by highlighting new screening methodologies for drug discovery that involve appropriate tagging of either substrate or the target protein itself with  $^{19}\text{F}$ -markers, that then report back on turnover and binding, respectively, via an the NMR screen. Taking this one step further, substrate-tagging with fluorine can be done in such a manner as to provide stereochemical information on enzyme mechanism. For example, substitution of one of the terminal hydrogens in phosphoenolpyruvate, provides insight into the, otherwise latent, facial selectivity of C-C bond formation in KDO synthase. Perhaps, most importantly, from the point of view of this discussion, appropriately tailored fluorinated functionality can be used to form to stabilized “transition state analogue” complexes with a target enzymes. Thus, 5-fluorinated pyrimidines,  $\alpha$ -fluorinated ketones, and 2-fluoro-2-deoxysugars each lead to covalent adduction of catalytic active site residues in thymidylate synthase, serine protease and glycosidase enzymes, respectively. In all such cases,  $^{19}\text{F}$  NMR allows the bioorganic chemist to spectrally follow “transition state analogue” formation. Finally, the use of specific fluorinated functionality to engineer “suicide substrates” is highlighted in a discussion of the development of the  $\alpha$ -(2' $^{\prime}\text{Z}$ -fluoro)vinyl trigger for amino acid decarboxylase inactivation. Here  $^{19}\text{F}$  NMR allows the bioorganic chemist to glean useful partition ratio data directly out of the NMR tube.

### 1. Introduction

The C-F bond is one of the strongest covalent bonds available, with an average bond energy of approximately 105–116 kcal/mol. This contributes significantly to the relative metabolic inertness of carbon-fluorine bonds, particularly those at unactivated  $\text{sp}^2$ -carbon-centers. Moreover, introduction of a C-F bond imposes only modest steric constraints, as the C-F bond (1.41–1.47 Å) is slightly shorter than a C-OH bond (1.52 Å) [1]. And while fluorine is the most electronegative element in the periodic table, it also has a very small atomic radius, resulting in an exceptionally low polarizability. DiMaggio has pointed out that this feature of organically-bound fluorine means that fluoroalkyl are less able to engage in dispersion-based interactions

Correspondence to: David B. Berkowitz.

**Publisher's Disclaimer:** This is a PDF file of an unedited manuscript that has been accepted for publication. As a service to our customers we are providing this early version of the manuscript. The manuscript will undergo copyediting, typesetting, and review of the resulting proof before it is published in its final citable form. Please note that during the production process errors may be discovered which could affect the content, and all legal disclaimers that apply to the journal pertain.

with aqueous solvent than simple alkyl groups. He has proposed the term, “polar hydrophobicity” [2] to describe this phenomenon, and points out that this may provide unique opportunities for enhancing ligand binding to a protein target [3]. In terms of specific interactions with functionalities in proteins, while C-F bonds appear to have rather limited H-bond acceptor ability [4–6], in optimally aligned cases F--H-N-amide interactions may make contributions to binding [7–9]. Additionally, more recent observations by Diederich and Müller [10–12] suggest that the hard C-F bond is able to engage amide carbonyls in specific attractive interactions reminiscent of the sort of trajectory-dependent  $n-\pi^*$  (amine-carbonyl) interactions suggested by Bürgi and Dunitz years before [13,14]. Finally, in the context of ionizable groups, such as fluorinated phosphonates as phosphate surrogates, one can use position and degree of organic fluorination to finely tune the  $pK_a$  of the surrogate [15]. Thus, the  $\alpha$ -monofluorophosphonates are generally “isoacidic” with the phosphate monoesters that they mimic [16,17]. For all of these reasons, incorporation of fluorinated functionality into ligands directed at protein targets is often advantageous, and will likely remain an important stratagem in medicinal chemistry for years to come [9,18–21]. An interesting new development along these lines involves the incorporation of the  $SF_5$ -group, in place of  $CF_3$  groups, for example, as has been put forth by Welch [22].

It is the purpose of this article to focus on the advantage offered by specific fluorinated functional groups, in both inhibitor design, and in mechanistic analysis. In this regard, emphasis will be placed on the possibility of observing protein-ligand interactions through the use of  $^{19}F$  NMR, and on the development of organofluorine functional groups to target active sites of interest, based upon an understanding of mechanism. We will begin with examples in which fluoroorganics are strategically introduced to serve as NMR-based reporting elements to provide (i) the medicinal chemist with a rapid screen for enzyme inhibition; (ii) the functional proteomics investigator with an assay for function and (iii) the mechanistic enzymologist with information on the stereochemical course of a biocatalytic reaction. From there, our discussion will move into organofluorine functionalities that have been specifically tailored to produce either transition state analogue inhibition or irreversible, enzyme-activated inhibition (i.e. suicide substrates).

## 2. Emergence of $^{19}F$ -Based NMR Screens for Inhibitor Development and Functional Proteomics

The past decade or so has seen the coming of age of NMR spectroscopy as a screening tool to facilitate the drug discovery process. This is particularly due to the influential work of Fesik and coworkers in developing so-called SAR by NMR techniques [23,24]. The last few years have seen the emergence of a number of creative  $^{19}F$ -based NMR techniques, that while philosophically similarly motivated, highlight the utility of fluorinated functionality in such systems. Notable advantages of the fluorine nucleus include its virtual “bio-orthogonality” [25], and its responsiveness to environmental factors. This is particularly true if one considers fluorination of an enzymatic substrate. The  $^{19}F$  isotropic chemical shift is very sensitive to small structural perturbations, resulting in chemical shift changes with substrate turnover, even in cases where the label is distal to the site of the chemistry. Moreover, if one employs  $CF_3$  groups as tags, one increases sensitivity, generating sharp singlets in the  $^{19}F$  spectrum and obviating the need for proton-decoupling, so long as the  $CF_3$  groups are not scalar-coupled to  $^1H$  nuclei. Thus, trifluoromethylated aromatics are ideal platforms for such applications.

This area has really blossomed in past several years, due in no small part to the work of Dalvit and co-workers [26]. As is shown in Figures 2 and 3, for screens of enzyme activity on peptide substrates this technique is particularly well-suited. If one employs trifluoromethylated aromatic amino acids, a single  $CF_3$  group suffices to yield clean assays for both peptide

phosphorylation, by AKT kinase in this case, or peptide cleavage, by trypsin here. Note that the fluorinated reporting amino acid does not itself undergo chemical transformation for either reaction being screened. Because CF<sub>3</sub> groups are employed for the reasons elaborated above, Dalvit labels this method 3-FABS (3 Fluorine Atoms for Biochemical Screening) [27]. A similar approach has been taken by Giralt and coworkers to screen for HIV protease inhibitors [28]. Quite recently, the Dalvit group has pointed out that the installation of reporting amino acids with two symmetrically disposed CF<sub>3</sub> groups (Fig. 2) increases sensitivity [29]. Indeed, his group has shown that sensitivity can be improved still further through the application of cryoprobe technology. These studies have established the ability of such CF<sub>3</sub>-tagged substrate methods to yield accurate IC<sub>50</sub> values. Thus, the 3-FABS approach is expected to see wider application for inhibitor screening, in automated manifolds, particularly in combinatorial chemistry applications.

In addition to this, one of the most promising observations to arise from this work is the notion that one might be able to generate a library of tagged substrates to probe for protein function. Thus, the tetradecapeptide illustrated in Figure 1 gives unambiguous and distinct signature signals for its specific phosphorylation by AKT kinase, and for its cleavage by trypsin (Note that though up to four potential tryptic cleavage sites are present, one appears to be preferred). When used as a test substrate for the PAK-4 protein, one sees the signature of serine-kinase activity. It remains to be seen how many such test peptide/signature reactions can be screened in parallel, perhaps in a single NMR tube, but the possibilities are intriguing, to be sure. One can imagine, for example, given optimal chemical shift dispersion, rapidly getting a fingerprint for the substrate specificities of newly isolated kinases, phosphatases, proteases or perhaps even histone acetyltransferases and/or histone deacetylases, by such methods. A principal advantage of such <sup>19</sup>F-based functional proteomics techniques is the near “bio-orthogonality” of carbon-bound fluorine [25].

### 3. Use of Fluorinated Functionality to Reveal Latent Enzyme Stereochemistry

Furdui, Anderson and coworkers have provided an elegant current example of how fluorine can be employed as analytical tool to study enzyme mechanism, even illuminating otherwise latent issues of pi-facial selectivity. Thus, both E- and Z-isomers of 3-fluoro-PEP serve as substrates for the enzyme KDO (3-deoxy-D-manno-2-octulosonate) 8-phosphate synthase [30]. And while the product stereochemistry requires that the key C-C-bond forming step involve attack of the nucleophilic-PEP 3-carbon upon the *re*-face of D-arabinose 5-phosphate, any facial selectivity with respect to PEP would be invisible here. As can be seen in the <sup>19</sup>F NMR spectrum of this enzymatic reaction (Fig. 3), *Aquifex pyrophilus* KDO8PS takes the E-isomer (−138 ppm) of 3-fluoro-PEP noticeably faster than the Z-isomer (−150 ppm), and, in so doing, catalyzes an aldol condensation at what would correspond to the *si*-face of the PEP substrate. This can be clearly seen from the NMR spectrum, as the new product carries the spectroscopic signature of authentic (3R)-fluoro-KDO-8P (δ<sup>19</sup>F @ −206 ppm). Interestingly, this *A. pyrophilus* enzyme and the KDO8PS from *E. coli* display the same facial selectivity for PEP and the same preference for the E-fluorinated compound, though they belong to different mechanistic classes, with only the latter being metal-dependent.

### 4. Use of Fluorinated Functionality for “Transition State Analogue” Inhibition

Particular advantage is offered by carefully crafted fluorinated functional groups that, at once, are able to trap out enzyme bound species resembling intermediates or “transition states.” Though the term “transition state analogue” used here must be understood figuratively, it has become common parlance in the field. Even in the most apropos cases, the term is a bit of an oxymoron, when one thinks about the concavity of a free energy surface. A true transition state mimic would sit at a concave downward point on that surface, whereas for tight-binding

inhibition, the E-TS analogue complex must rest in a free energy well, i.e. in a concave upward region. That said, in some cases, one, in fact, succeeds in forming a reversible covalent enzyme-inhibitor complex that resembles a high energy intermediate along the normal enzymatic reaction coordinate, but for which no productive pathway forward (to product) is available. And, by a Hammond postulate argument, mimicking a high energy intermediate perhaps justifies the label “transition state” analogue. This could be said of the  $\alpha$ -fluorinated ketone inhibitors for serine proteases discussed below, as well as for the 2-fluoro-sugar glycosidase inhibitors. In all of the cases presented here, fluorination serves the dual purpose of finely tuning the functional group to form a stable complex with the target enzyme, and of providing a unique spectroscopic window through which the bioorganic chemist can follow and characterize for the formation of this complex.

#### 4.1 $\alpha$ -Trifluoromethyl Ketones as Serine Protease Inhibitors

Robert Abeles and coworkers pioneered the use of  $\alpha$ -fluorinated ketones as serine protease inhibitors. In this design, the  $\alpha$ -CF<sub>n</sub> substituent destabilizes the C-O  $\pi$ -bond to which it is attached. This renders the carbonyl susceptible to hydration, and to addition of the active site serine, when incorporated into a suitable peptide scaffold, mimicking a typical substrate (Fig. 4). The resultant hemiacetal addition complex represents an analogue of the tetrahedral intermediate formed upon the normal reaction coordinate for enzymatic peptide bond cleavage. A secondary effect of the fluoroalkyl substituent is to lower the hemiacetal pK<sub>a</sub> for this tetrahedral intermediate (vide infra for <sup>19</sup>F NMR titration). This, in turn, insures essentially complete oxyanionic character of the addition complex, promoting favorable interactions with the active site “oxyanion hole.”

An early study by Imperiali and Abeles [31] established that for N-acetyl-leucine-phenylalanyl-fluoroketone dipeptide mimics, both the percent hydration and the potency of chymotrypsin inhibition correlate nicely with the extent of  $\alpha$ -fluorination. Thus, <sup>19</sup>F NMR established that the  $\alpha$ -monofluoroketone is approximately 50% hydrated, whereas the di- and trifluoroketones are ~100% hydrated in aqueous solution. K<sub>i</sub> decreases from 200 to 25 to 1 micromolar, in this series. Subsequent work showed it possible to monitor the formation of the active site serine adduct by <sup>19</sup>F NMR [32]. Comparison of chemical shifts with those of model compounds was consistent with hemiketal formation (Fig. 5).

Moreover, pH titration of the E-I complex, as monitored by <sup>19</sup>F NMR (Fig. 6.), allowed for experimental estimation of the bound,  $\alpha$ -fluorinated hemiketal pK<sub>a</sub> at 4.9 [32,33]. Thus, the  $\alpha$ -fluorinated hemiketal pK<sub>a</sub> is apparently lowered by approximately 4 log units, in the active site, suggestive of favorable interactions in the oxyanion hole. These studies firmly established the utility of such fluorinated functionality, both to trap out a stable mimic of the E-S tetrahedral intermediate, and as an analytical tool providing a <sup>19</sup>F beacon, allowing the experimentalist to monitor the formation of this binary complex and its chemical environment. The work built on earlier studies by Shah and Gorenstein, that established <sup>19</sup>F NMR as an analytical tool to monitor transition state analogue formation with peptidyl aldehydes in which a <sup>19</sup>F tag had been inserted at the p-position of a phenylalanine ring [34,35].

More recently, the structural details of this protein-bound hemiketal presaged by these nice, NMR-assisted bioorganic studies, have been revealed by X-ray crystallographic studies of the complex [36]. The canonical Ser-195-His-57-Asp-102 catalytic triad is highlighted in Figure 7, with the former residue clearly having added in to the activated carbonyl center. Later, a higher resolution structure of this same complex and the analogous chymotrypsin-N-Ac-phenylalanine-COF<sub>3</sub> complex [37] were taken as structural evidence by Frey and coworkers for a “low barrier hydrogen-bond (LBHB)” postulated to form in the chymotrypsin transition state. Specifically, the observed  $\delta$ -N-His(57)- $\delta$ -O-Asp(102) distance of 2.6 Å is less than the sum of the van der Waals radii of N and O (2.7 Å), thereby meeting the definition of a LBHB.

More recently, Warshel has called this view of the complex into question, concluding rather that one is seeing tight complexation here as result of dipole preorganization by the protein [38]. All of these studies highlight the value of this fluorinated functionality in mechanistic enzymology, providing insight into factors stabilizing the enzymatic transition state.

Trifluoromethyl ketone inhibitors of other serine proteases, such as elastase and  $\alpha$ -lytic protease [39] and the notable cardiovascular target chymase [40,41] have been developed. A related *a,a*-difluoropyruvamide motif is also quite effective in the chymotrypsin active site, as illustrated in Figure 5. The fluorinated ketone transition state analogue approach can be extended to the inhibition of serine esterases, including acetylcholinesterase [42] and phospholipase A2 [43].  $^{19}\text{F}$  NMR can be applied to this class of enzymes as well, to observe E-I complex formation [44]. Interestingly, the zinc-metalloproteases carboxypeptidase A and angiotensin converting enzyme [45] are also susceptible to inhibition based upon this design [46].

#### 4.2 5-Fluorodeoxyuridylate Monophosphate and Thymidylate Synthase

Over the last 25 years, 5-fluorouracil (5-FU) has seen widespread clinical application, in chemotherapy, particularly for colorectal cancer [47]. On the one hand, 5-fluorouracil does get incorporated into both nucleosides and 2'-deoxynucleosides and these nucleosides are fully phosphorylated to the 5'-triphosphates. This leads to the incorporation of 5-FU into both DNA and RNA. However, incorporation into nucleic acid does not generally correlate with effectiveness as a chemotherapeutic agent [48]. On the other other hand, the key 5-FU metabolite, 5-fluoro-dUMP acts, as designed, as an effective inhibitor of the enzyme, thymidylate synthase (TS). This enzyme normally catalyzes the one carbon transfer from  $\text{N}^5, \text{N}^{10}$ -methylene-tetrahydrofolate ( $\text{CH}_2$ -THF) to the 5-position of dUMP, producing thymidine-5'-monophosphate and dihydrofolate (DHF). This is an essential step in pyrimidine biosynthesis, and the effectiveness of 5-FU as a chemotherapeutic generally correlates well with TS levels in the target tumor, and with effectiveness in TS activity knockdown upon treatment.

The 5-fluoro-dUMP system is also one of the earliest in which a mechanistically important fluorine atom would report back to the bioorganic chemist on inhibition mechanism. By design, 5-fluorination should promote the conjugate addition of the active site cysteine and allow for the capture of the resultant  $\alpha$ -fluoro-enolate with the iminium ion derived from  $\text{CH}_2$ -THF (Fig. 8.). However, the accepted mechanistic third step,  $\alpha$ ,  $\beta$ -elimination of THF, would necessarily be prevented by  $\alpha$ -fluorination. This, by design, should lead to the build-up of a covalent E-I- $\text{CH}_2$ -THF complex. Indeed, as early as 1976, James, Santi and co-workers described  $^{19}\text{F}$  NMR evidence of a successful adduction of the active site nucleophile via conjugate addition [49]. These studies were performed on an peptide fragment of the protein that included the adducted active site cysteine.

Several years later, an elegant series of studies by Dunlap and co-workers with the intact thymidylate synthase (TS) protein [50–53] demonstrated that one could follow and differentiate the formation of (i) binary (E-FdUMP); (ii) pseudo-ternary (E-FdUMP + THF) and (iii) covalent ternary (E-FdUMP- $\text{CH}_2$ -THF) complexes by  $^{19}\text{F}$  NMR. The spectroscopic signatures for these complexes are provided in Figure 8. Comparison with the  $^{19}\text{F}$  NMR spectrum of the bisulfite adduct of 5-fluoro-dUMP guided the original assignment of the covalent, binary adduct as the 5,6-dihydro derivative of the fluorinated pyrimidine. Independent determinations of the three dimensional structure for the covalent ternary complex with the *E. coli* enzyme have been provided from the groups of Matthews and Montfort. A rendering of the latter structure with VMD [54] is presented in Fig. 8., demonstrating clearly that the ternary complex has been arrested, following conjugate addition of cysteine-146 and THF-methylenation, as designed.



### 4.3 Fluoro-sugars as Glycosidase Inhibitors

The Withers group has introduced a strategy for inhibiting glycosidases that exploits an  $\alpha$ -fluoro effect not unlike that established by Abeles in the serine protease arena (vide supra). A common feature of “retaining glycosidases” is that they are believed to proceed via the intermediacy of a covalent E-S complex. Moreover, both the formation and hydrolysis of the glycosyl enzyme species proceed via transition states with considerable oxocarbenium ion character. Thus,  $\alpha$ -fluorination, just as for a carbonyl center, is expected to destabilize this onium species, slowing both the rates of glycosyl enzyme formation and breakdown. However, the inclusion of a reactive leaving group, such as dinitrophenol or fluoride at the anomeric center of the inhibitor serves to accelerate formation of the glycosyl enzyme intermediate with these inhibitors. Once formed, the adduct is greatly stabilized by the presence of the 2-fluoro-substituent. Such activated 2-deoxy-2-fluorosaccharides have now been shown to trap out active site carboxylate residues in a number of glycosidase active sites. The original work was carried with  $\beta$ -glucosidase [55–57], and both the formation of an active site 2-deoxy-2-fluoroglucoside, and its  $\alpha$ -stereochemistry were established by  $^{19}\text{F}$  NMR. Figure 9 illustrates a more recent example in which one observes the capture of glutamate-233, with the  $\alpha$ -anomeric stereochemistry, in the active site of  $\beta$ -glucanase via  $^{19}\text{F}$  NMR [58]. Subsequent solution of the three dimensional X-ray structure of the E-I complex confirmed these assignments.

The same principle has now been applied to the inhibition of lysozyme [59], as well as xylanase [60], galactosidase [61], mannosidase [62] enzymes. More recent studies indicate that sialidase enzymes, important bacterial, viral and trypanosomal targets, are also effectively adducted with fluorinated neuraminic acids [63]. Here, X-ray crystallography has indeed, established that the trapped out active site residue is a tyrosine, rather than a glutamate or aspartate residue [64–66]. Even beyond this, success has been achieved in inhibiting 1,3-fucosyltransferase, for example, with guanosine 5'-diphospho-2-deoxy-2-fluoro-beta-L-fucose (GDP-2F-Fuc) [67], suggesting that the Withers approach to the inhibition of glycosyl hydrolase enzymes may be quite broadly extensible to the domain of glycoside synthesis enzymes, as well.

## 5. Use of Fluorinated Functionality for “Suicide Substrate” Inactivation

Quite a number of tailored fluorinated functional groups serve as the basis for the suicide inactivator development. Among the most notable examples are  $\alpha$ -difluoromethylornithine (DFMO), a mechanism-based inactivator of L-ornithine decarboxylase (ODC), the enzyme that controls flux through the polyamine pathway, associated with cell growth and differentiation. Inactivation of this enzyme proceeds via pyridoxal phosphate (PLP)-assisted decarboxylative elimination of fluoride to produce an fluorinated Michael acceptor, that is captured by an active site cysteine residue. This has been established by both mass spectrometric [68] and x-ray crystallographic studies [69] from the groups of Pegg and Phillips, respectively. DFMO inhibition of trypanosomal ODC cures African Sleeping Sickness [70]. The compounds is also under clinical evaluation for the prevention of colon cancer [71,72].

Gemcitabine, 2'-deoxy-2',2'-difluorocytidine, is widely used in the treatment of advanced pancreatic cancer. The compound is a pro-drug, being 5'-phosphorylated in vivo. The triphosphate is a DNA polymerase chain terminator, whereas the diphosphate is a suicide substrate for ribonucleotide reductase, an enzyme that operates via a radical mechanism, using an active site tyrosyl radical. Fluoride's leaving group ability from an electron rich system, once again, is exploited here [73].

Like DFMO,  $\alpha$ -monofluorinated amino acids, can be used as suicide substrates for PLP-dependent enzymes, and, once again the leaving group ability of fluoride is important in the inactivation mechanism, in this case. However, the monofluoromethyl trigger generally leads to an enamine-based nucleophilic inhibition mechanism [74,75] first observed by Metzler with

serine O-sulfate [76,77]. Another notable PLP enzyme inactivator is  $\alpha$ -(1'-fluoro)vinylglycine, a suicide substrate for both bacterial alanine racemase [78,79] and for tryptophan synthase [80]. Once again, the ability of fluoride to leave from an electron rich intermediate is exploited, presumably leading to an allenic imine, following enzymatic  $\alpha$ -deprotonation, as originally proposed by Abeles.

Finally, the use of o- or p-(di)fluoromethylphenoxy or thiophenoxy leaving groups, as precursors to (halo)quinone methides has also been exploited in phosphatase, glycosidase and amidase active sites by the groups of Widlanski [81–83], Danzin [84] and Badet [85–87], respectively. Recently, Thompson has shown that arginine deiminase enzymes can be effectively targeted utilizing a fluorinated acetamidine functionality [88,89].

That said, the discussion here will focus on work in these laboratories, specifically on the development of the  $\alpha$ -(2'Z-fluoro)vinyl trigger for PLP-dependent amino acid decarboxylase (AADC) inactivation. This approach evolved from initial efforts to stereoselectively install the simple, unsubstituted  $\alpha$ -vinyl trigger, itself.  $\alpha$ -Vinylglycine is a naturally occurring inactivator of number of PLP-dependent enzymes [90], including transaminases and ACC (1-amino-1-cyclopropanecarboxylate) synthase [91]. The natural occurrence of this Trojan horse functionality presumably inspired its incorporation into  $\gamma$ -vinyl-GABA (Vigabatrin), an effective GABA transaminase inactivator [92,93], and anti-convulsant drug. In both of these cases, x-ray crystallographic studies [92,91] have now confirmed that the active site lysine is captured, presumably via conjugate addition to an  $\alpha$ ,  $\beta$ -unsaturated iminium ion, following enzyme-mediated azallylic isomerization.

If one wishes to use such a  $\pi$ -trigger to selectively target PLP-dependent AADC's, as opposed to transaminase, racemase, eliminase or replacement enzymes, then substitution of the  $\alpha$ -proton with the vinylic functionality appears to be a good design. This design eliminates the possibility of  $\alpha$ -deprotonation [as opposed to situating the  $\pi$ -trigger along the side chain or in place of the  $\alpha$ -carboxylate (product analogue)], but still allows for  $\alpha$ -decarboxylation, thereby potentially conferring specificity. This design also likely promotes errant protonation, following decarboxylation, another potential advantage discussed below.

With these design advantages, however, comes a synthetic challenge. One must construct quaternary  $\alpha$ -vinyl amino acids, ideally with control of stereochemistry at this quaternary center. Because of the accessibility of amino ester-based enolates, two disconnections are most attractive here, either installation of the vinyl group, via formal vinylation of the enolate derived from the cognate amino acid (AA), or installation of the side chain, via formal alkylation of a vinylglycine enolate equivalent. Initially, we chose the former approach, finding that N-benzoyl-protected amino acid esters could be doubly deprotonated and selectively  $\alpha$ -alkylated with ethylene oxide, as vinyl cation equivalent [94,95]. Pleasingly, one could carry the protected side chains of even highly functionalized AA's (His, Lys, Orn, hSer, DOPA) into these dianions, suggesting broader application of such an approach to the synthesis of  $\alpha$ -alkylated AA's, in general. Of course, these quaternary,  $\alpha$ -vinyl AA's, though rapidly assembled, are obtained in racemic form. Coupling this chemistry with an enzymatic resolution via "reverse transesterification" [96] provided a partial, though incomplete, solution to this stereochemical problem.

We next turned to the converse approach, beginning with vinylglycine equivalent and installing the side chain via stereoselective alkylation. On the one hand, we found that N-benzoyl-L- $\alpha$ -vinylglycine methyl ester, available from L-homoserine lactone [97], could be effectively cyclized to the corresponding L-cis and trans-oxazolines, under the aegis of a "PhSe<sup>+</sup>" equivalent, without loss of absolute stereochemistry (Fig. 10). Separation of these diastereomeric oxazolines give both a D- $\alpha$ -vinyl AA synthon (cis) and an L- $\alpha$ -vinyl AA



synthon (trans) [98]. This is because one sees essentially absolute 1,2-stereoinduction in the alkylation event that introduces the AA side chain. Because one destroys the original  $\alpha$ -stereocenter in this step, and exploits the newly installed  $\beta$ -stereocenter to direct the  $\alpha$ -alkylation, one may regard this as a “self-reproduction of chirality” [99–101] or a “self-regeneration of stereocenters” approach [102], terms introduced by Seebach. One then unmasks the  $\alpha$ -vinyl group through a sequence involving elimination (E2 conditions) to the  $\alpha$ -(2'E-phenylseleno)vinyl AA, selenium-tin interchange and proto-destannylation. The intermediate conversion of a terminal vinyl selenide to a terminal vinylstannane constituted a fundamentally new method for vinylstannane synthesis. Moreover, the resultant, protected  $\alpha$ -(2'E-tributylstannyl)vinyl AA's could be exploited as building blocks for the construction of  $\alpha$ -branch-extended analogues via Pd-mediated cross coupling chemistry [103]. For all of its versatility, this route has the limitation that only particularly reactive  $S_N2$  electrophiles can be efficiently captured in the oxazoline enolate alkylation step.

As a solution to this enolate reactivity issue, a complementary approach to the stereocontrolled synthesis of quaternary  $\alpha$ -vinyl amino acids was developed. Namely, the AA side chain is introduced via alkylation of a chiral vinylglycine-derived dianionic dienolate, bearing a  $\beta$ -naphthylmenthyl ester auxiliary (Fig. 11) [104]. Enolate geometry is presumably controlled via amidate nitrogen chelation to lithium, and facial selectivity follows an “exo-extended” model for the reactive conformation of the dienolate. High levels of acyclic stereocontrol are achieved, even for unreactive  $S_N2$  electrophiles. Moreover, given Comins' enzyme resolution technology [105], both antipodes of the requisite (desmethyl) chiral auxiliary are available, providing access to either antipode of the target quaternary  $\alpha$ -vinyl AA. More recently in the group, good progress has been made toward transition metal-mediated routes into these densely functionalized  $\beta$ ,  $\gamma$ -unsaturated AA's, with the potential for catalytic control of stereochemistry. This includes both allylic amination [106–108] and formal [3,3]-sigmatropic rearrangement approaches [109].

It is important to point out at this stage that the vinyl AA's themselves serve as precursors to other  $\alpha$ -branched AA's with potential as enzyme inactivators, including  $\alpha$ -oxiranyl [110],  $\alpha$ -chlorovinyl [111] and  $\alpha$ -bromovinyl AA's. But, most importantly here, we were able to demonstrate that protected, enantiomerically enriched,  $\alpha$ -vinyl AA's, available from the chemistry described in Figs. 10 and 11, could be smoothly transformed into the corresponding  $\alpha$ -(2'Z-fluoro)vinyl AA's, with preservation of stereochemical purity [112]. As outlined in Figure 12, this transformation involves an ozonolysis/fluoromethylenation sequence, that avails itself of the McCarthy reagent [113,114].

In light of earlier success with the simple  $\alpha$ -vinyl trigger and *Hafnia alvei* L-lysine decarboxylase (LDC) [115], we set to examine the  $\alpha$ -(2'Z-fluoro)vinyl trigger [116,117] for AADC inactivation in this active site. Figure 13 illustrates the proposed mechanism(s) of AADC inactivation with this new AADC suicide substrate trigger. Transaldimination is expected to give external aldimine **I**, thereby releasing the enzymatic lysine from the internal aldimine linkage. Decarboxylation, the normal second mechanistic step, then provides the quinonoid intermediate, **II**. While the previously isolated fluorovinyl group is now conjugated with the extended  $\pi$ -system of the cofactor, it is not very electrophilic, as it possesses, at once,  $\alpha$ ,  $\beta$ -unsaturated iminium ion and tetra-enamine substructures. In the third step, protonation at any of three available sites would restore pyridinium ion aromaticity. On the one hand,  $\alpha$ -protonation would re-isolate the fluorovinyl group, and represents the simple turnover pathway. However,  $C_4$ -protonation would have the effect of protonating the tetra-enamine substructure, thereby producing a potent electrophile, the  $\beta$ -fluoro- $\alpha$ ,  $\beta$ -unsaturated iminium ion **IV**. In this species, the  $\beta$ -fluoro substituent serves the dual role of increasing the electrophilicity of the Michael acceptor, and potentially serving as a leaving group, transforming what would be a conjugate addition mechanism with a simple vinyl trigger into an addition-elimination

mechanism with the fluorovinyl trigger. Finally, protonation at the  $\gamma$ -position should lead to release of an enamine-type product, **VIII**, that, most likely would either undergo Mannich condensation with the internal aldimine (Metzler mechanism [76,77]) or expel the  $\gamma$ -fluoride leaving group. This latter pathway would give a second electrophile, **X**, a potentially diffusible  $\alpha$ ,  $\beta$ -unsaturated iminium ion.

Note that errant protonation (i.e.  $C_{\alpha'}$ - and/or  $\gamma$ -protonation) is thus required, by design, for inactivation with this trigger. Consistent with this requirement, early studies by O'Leary and others on AADC mechanism reveals that  $\alpha$ -substitution, specifically, replacement of the  $\alpha$ -proton with a methyl substituent, tends to promote  $C_{\alpha'}$  protonation. Thus, this so-called abortive transamination pathway is known to be increased by 1–2 orders of magnitude upon  $\alpha$ -methylation [118–121]. As noted, this validates placement of this  $\pi$ -trigger at the  $\alpha$ -carbon, so as to create steric hindrance to  $\alpha$ -protonation there. Note further that errant protonation is expected to lead to release of fluoride ion, either (i) prior to enzyme alkylation ( $\alpha$ ,  $\beta$ -unsaturated iminium ion pathway), (ii) concomitant with enzyme alkylation ( $\beta$ -fluoro- $\alpha$ ,  $\beta$  unsaturated iminium ion pathway) or (iii) subsequent to enzyme adduction (Metzler enamine pathway). This means that  $^{19}\text{F}$  NMR should allow the experimentalist to directly monitor partitioning in the protonation step itself.

An enantioselective synthesis of each antipode of  $\alpha$ -(2'*Z*-fluoro)vinyllysine (FVL) was achieved as outlined in Figures 11 and 12 [122]. 4-Iodo-N-SES-N-PMB-butylamine was used as the  $\text{S}_{\text{N}}2$  electrophile for introduction of the lysine side chain. Examination of the individual FVL-antipodes shows the D-enantiomer to be exclusively a substrate, whereas the L-antipode is a suicide substrate, displaying time dependent inactivation of LDC. A Kitz-Wilson analysis of the data for L-FVL, yields  $k_{\text{inact}} = 0.26 \pm 0.07 \text{ min}^{-1}$  and  $K_{\text{I}} = 86 \pm 22 \text{ mM}$ . This is comparable to the  $k_{\text{inact}}$  values seen for both antipodes of DFMO and (S)-Vigabatrin. The  $K_{\text{I}}$  value is significantly higher than that seen for L-DFMO ( $\sim 1.3 \text{ mM}$ ) [123], but significantly lower than that seen for (S)-Vigabatrin ( $\sim 3 \text{ mM}$ ) [124]. Inactivation was seen to be functionally irreversible (exhaustive dialysis). Curvature in  $\ln(E_t/E_0)$  vs.  $t$  plots was observed, suggestive of significant partitioning into natural or unnatural turnover pathways. A titration of the enzyme, with varying I:E ratios, provided an estimate of the partition ratio (total turnovers per inactivation event) of  $\sim 20 \pm 3$ .

Independent synthesis of  $\alpha$ -(2'*Z*-fluoro)vinylcadaverine (FVC) established the viability of following the enzymatic reaction course by  $^{19}\text{F}$  NMR (see Fig. 14 and the FVC- and fluoride-spiking experiments shown). Inactivation of  $15 \mu\text{M}$  LDC produces  $168 \pm 14 \mu\text{M}$  turnover product (FVC) and  $70 \pm 13 \mu\text{M}$  fluoride. The fluoride value was confirmed with an ion-specific electrode ( $78 \pm 5 \mu\text{M}$ ). Since all errant protonations are projected to release fluoride, we can estimate that 1 in 3.2 decarboxylations leads to errant protonation (29%!), with 1 in 5 errant protonation events leading to LDC inactivation. This gives an overall partition ratio of  $16 \pm 2$ . The high errant protonation rate ( $\sim 8$  times the maximum value produced by  $\alpha$ -methylation) seen in this model AADC active site is promising, as, by design, altered protonation is required for trigger actuation. Given this and the favorable  $k_{\text{inact}}$ , it will be of interest to examine this trigger in other AADC active sites. The remarkable enantiodiscrimination observed contrasts with the case of DFMO, in which similar behavior has been reported for both antipodes [123].

In summary, synthetic chemistry has been developed that allows for the enantioselective construction of quaternary amino acids, outfitted with an  $\alpha$ -(2'*Z*-fluoro)vinyl trigger. In the first test of this trigger, in the LDC active site, one sees both efficient enzyme inactivation, and the fringe benefit of the  $^{19}\text{F}$  beacon, built into the trigger. Thus,  $^{19}\text{F}$  NMR can be exploited to provide information on trigger partitioning, particularly in the important quinonoid protonation step. Thus, whereas the traditional titration experiment provides information on the number of

inhibitor molecules “turning over” per inactivation event, it provides no information on how those turnovers take place. The  $^{19}\text{F}$  experiment supplies additional fine structure, showing here that approximately 30% of those turnovers do result in the desired errant protonation, with the remaining 70% going on to the usual decarboxylation product ( $\alpha$ -protonation). This example, when considered along with the fluoromethyl ketone (serine proteases), 5-fluoropyrimidine (thymidylate synthase) and 2-deoxy-2-fluoro-sugar (retaining glycosidases and glycosyl transferases) cases discussed earlier in this article, highlights the dual utility of appropriately tailored fluorinated functionality, for both enzyme inhibition and the mechanistic study of that inhibition, in situ, with  $^{19}\text{F}$  NMR spectroscopy.

## Acknowledgments

We thank the NSF and the NIH (CA 62034 and RR016544-01) for support of unnatural amino acid synthesis, fluorinated trigger development and mechanism-based enzyme inhibition efforts in our laboratory.

## References

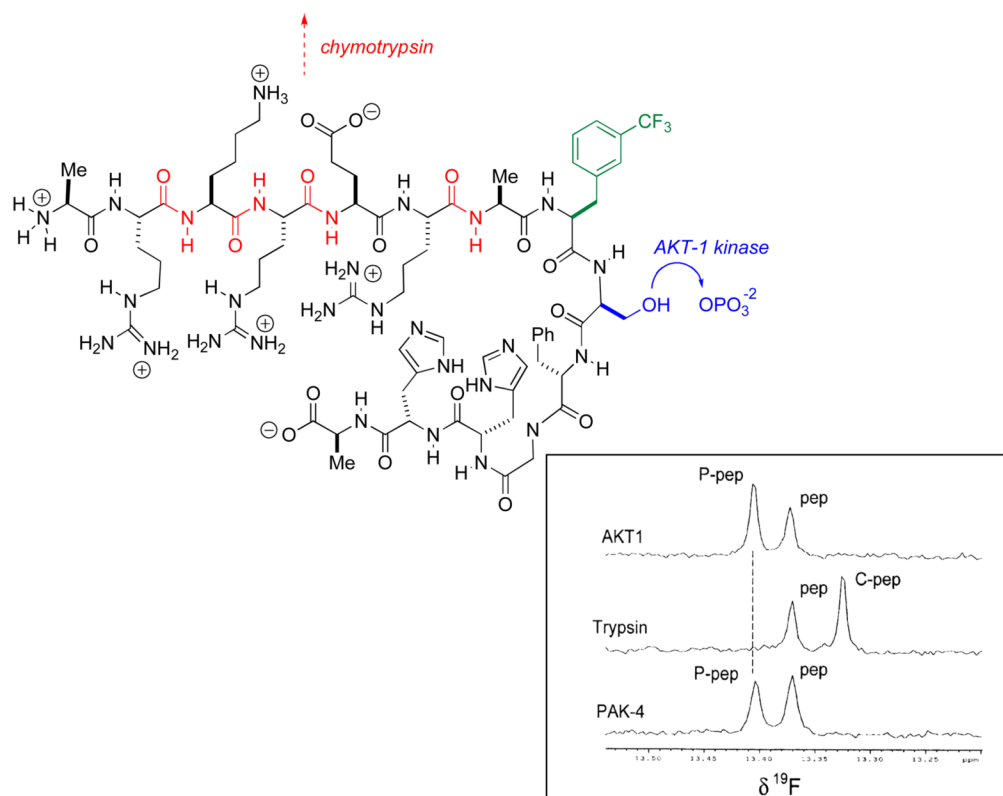
1. O'Hagan D. Chem Soc Rev 2008;37:308–319. [PubMed: 18197347]
2. Biffinger JC, Kim HW, DiMagno SG. ChemBioChem 2004;5:622–627. [PubMed: 15122633]
3. Kim HW, Rossi P, Shoemaker RK, DiMagno SG. J Am Chem Soc 1998;120:9082–9083.
4. Plenio H, Diodone R. Chem Ber/Recl 1997;130:633–640.
5. Dunitz JD, Taylor R. Chem--Eur J 1997;3:89–98.
6. Howard JAK, Hoy VJ, O'Hagan D, Smith GT. Tetrahedron 1996;52:12613–12622.
7. Hyla-Kryspin I, Haufe G, Grimme S. Chem Eur J 2004;10:3411–3422.
8. Chen L, Wu L, Otaka A, Smyth MS, Roller PP, Burke TR Jr, den Hertog J, Zhang ZY. Biochem Biophys Res Commun 1995;216:976–984. [PubMed: 7488220]
9. Mueller K, Faeh C, Diederich F. Science 2007;317:1881–1886. [PubMed: 17901324]
10. Fischer FR, Schweizer WB, Diederich F. Angew Chem, Int Ed 2007;46:8270–8273.
11. Schweizer E, Hoffmann-Roder A, Scharer K, Olsen JA, Fah C, Seiler P, Obst-Sander U, Wagner B, Kansy M, Diederich F. ChemMedChem 2006;1:611–621. [PubMed: 16892401]
12. Paulini R, Mueller K, Diederich F. Angew Chem, Int Ed 2005;44:1788–1805.
13. Burgi HB, Dunitz JD, Shefter E. J Amer Chem Soc 1973;95:5065–5067.
14. Buergi HB, Dunitz JD. Acc Chem Res 1983;16:153–161.
15. Berkowitz DB, Bose M. J Fluorine Chem 2001;112:13–33.
16. Berkowitz DB, Bose M, Pfannenstiel TJ, Doukov T. J Org Chem 2000;65:4498–4508. [PubMed: 10959850]
17. Nieschalk J, Batsanov AS, O'Hagan D, Howard JAK. Tetrahedron 1996;52:165–76.
18. Kirk KL. Org Process Res Dev 2008;12:305–321.
19. Begue JP, Bonnet-Delpon D. Actualite Chimique 2006;301–302:83–87.
20. O'Hagan D, Rzepa HS. Chem Commun 1997:645–652.
21. Pongdee R, Liu H-w. Bioorg Chem 2004;32:393–437. [PubMed: 15381404]
22. Welch JT, Lim DS. Bioorg Med Chem 2007;15:6659–6666. [PubMed: 17765553]
23. Fesik SW, Shuker SB, Hajduk PJ, Meadows RP. Protein Eng 1997;10:73.
24. Shuker SB, Hajduk PJ, Meadows RP, Fesik SW. Science 1996;274:1531–1534. [PubMed: 8929414]
25. Dong C, Huang F, Deng H, Schaffrath C, Spencer JB, O'Hagan D, Naismith JH. Nature 2004;427:561–565. [PubMed: 14765200]
26. Dalvit C. Prog Nucl Magn Reson Spectrosc 2007;51:243–271.
27. Dalvit C, Ardini E, Flocco M, Fogliatto Gian P, Mongelli N, Veronesi M. J Am Chem Soc 2003;125:14620–14625. [PubMed: 14624613]
28. Frutos S, Tarrago T, Giralt E. Bioorg Med Chem Lett 2006;16:2677–2681. [PubMed: 16517158]

29. Papeo G, Giordano P, Brasca MG, Buzzo F, Caronni D, Ciprandi F, Mongelli N, Veronesi M, Vulpetti A, Dalvit C. *J Am Chem Soc* 2007;129:5665–5672. [PubMed: 17417847]
30. Furdui CM, Sau AK, Yaniv O, Belakhov V, Woodard RW, Baasov T, Anderson KS. *Biochemistry* 2005;44:7326–7335. [PubMed: 15882071]
31. Imperiali B, Abeles RH. *Biochemistry* 1986;25:3760–3767. [PubMed: 3527255]
32. Liang TC, Abeles RH. *Biochemistry* 1987;26:7603–7608. [PubMed: 3427096]
33. Brady K, Liang TC, Abeles RH. *Biochemistry* 1989;28:9066–9070. [PubMed: 2605240]
34. Shah DO, Gorenstein DG. *Biochemistry* 1983;22:6096–7101.
35. Gorenstein DG, Shah DO. *Biochemistry* 1982;21:4679–4686. [PubMed: 7138821]
36. Brady K, Wei A, Ringe D, Abeles RH. *Biochemistry* 1990;29:7600–7607. [PubMed: 2271520]
37. Neidhart D, Wei Y, Cassidy C, Lin J, Cleland WW, Frey PA. *Biochemistry* 2001;40:2439–2447. [PubMed: 11327865]
38. Schutz CN, Warshel A. *Proteins* 2004;55:711–723. [PubMed: 15103633]
39. Govardhan CP, Abeles RH. *Arch Biochem Biophys* 1990;280:137–146. [PubMed: 2353815]
40. Deguchi, T.; Shiratake, R.; Sato, F.; Fujitani, T.; Honda, Y.; Kiyoshi, A.; Notake, M.; Showell, GA.; Boyle, RG.; Klair, SS. Dainippon Pharmaceutical Co., Ltd; Japan: 2003. p. 44Application: JP JP
41. Deguchi, T.; Shiratake, R.; Sato, F.; Fujitani, B.; Kiyoshi, A.; Honda, Y.; Notake, M. Abstracts of Papers, 223rd ACS National Meeting; Orlando, FL, United States. April 7–11, 2002; 2002. MEDI-061
42. Allen KN, Abeles RH. *Biochemistry* 1989;28:8466–8473. [PubMed: 2605196]
43. Street IP, Lin HK, Laliberte F, Ghomashchi F, Wang Z, Perrier H, Tremblay NM, Huang Z, Weech PK, Gelb MH. *Biochemistry* 1993;32:5935–40. [PubMed: 8018213]
44. Rosell G, Herrero S, Guerrero A. *Biochem Biophys Res Commun* 1996;226:287–292. [PubMed: 8806628]
45. Natesh R, Schwager SLU, Sturrock ED, Acharya KR. *Nature* 2003;421:551–554. [PubMed: 12540854]
46. Gelb MH, Svaren JP, Abeles RH. *Biochemistry* 1985;24:1813–1817. [PubMed: 2990541]
47. Longley DB, Harkin DP, Johnston PG. *Nat Rev Cancer* 2003;3:330–338. [PubMed: 12724731]
48. Noordhuis P, Holwerda U, Van der Wilt CL, Van Groenigen CJ, Smid K, Meijer S, Pinedo HM, Peters GJ. *Annals of Oncology* 2004;15:1025–1032. [PubMed: 15205195]
49. James TL, Pogolotti AL Jr, Ivanetich KM, Wataya Y, Lam SSM, Santi DV. *Biochem Biophys Res Commun* 1976;72:404–410. [PubMed: 825116]
50. Lewis CA Jr, Ellis PD, Dunlap RB. *Biochem Biophys Res Commun* 1978;83:1509–1517. [PubMed: 100115]
51. Lewis CA Jr, Ellis PD, Dunlap RB. *Biochemistry* 1980;19:116–123. [PubMed: 6766311]
52. Lewis CA Jr, Ellis PD, Dunlap RB. *Biochemistry* 1981;20:2275–2285. [PubMed: 6786329]
53. Zapf JW, Weir MS, Emerick V, Villafranca JE, Dunlap RB. *Biochemistry* 1993;32:9274–9281. [PubMed: 8103678]
54. Humphrey W, Dalke A, Schulten K. *J Molec Graphics* 1996;14.1:33–38.
55. Withers SG, Rupitz K, Street IP. *J Biol Chem* 1988;263:7929. [PubMed: 3286645]
56. Wicki J, Rose David R, Withers Stephen G. *Methods Enzymol* 2002;354:84–105. [PubMed: 12418218]
57. Street IP, Kempton JB, Withers SG. *Biochemistry* 1992;31:9970–9978. [PubMed: 1390781]
58. White A, Tull D, Johns K, Withers SG, Rose DR. *Nat Struct Biol* 1996;3:149–154. [PubMed: 8564541]
59. Vocadlo DJ, Withers SG. *Carbohydr Res* 2005;340:379–388. [PubMed: 15680592]
60. Miao S, Ziser L, Aebersold R, Withers SG. *Biochemistry* 1994;33:7027–7032. [PubMed: 7911679]
61. Ly HD, Howard S, Shum K, He S, Zhu A, Withers SG. *Carbohydr Res* 2000;329:539–547. [PubMed: 11128583]
62. Howard S, He S, Withers SG. *J Biol Chem* 1998;273:2067–2072. [PubMed: 9442045]

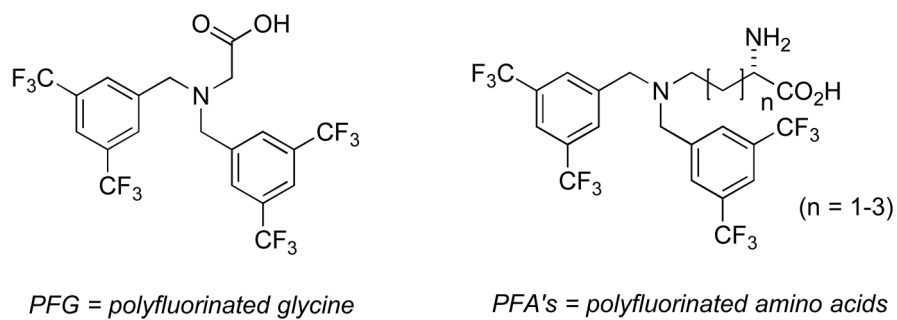
63. Watts AG, Damager I, Amaya ML, Buschiazzi A, Alzari P, Frasch AC, Withers SG. *J Am Chem Soc* 2003;125:7532–7533. [PubMed: 12812490]
64. Newstead SL, Potter JA, Wilson JC, Xu G, Chien CH, Watts AG, Withers SG, Taylor GL. *J Biol Chem* 2008;283:9080–9088. [PubMed: 18218621]
65. Watts AG, Oppezzo P, Withers SG, Alzari PM, Buschiazzi A. *J Biol Chem* 2006;281:4149–4155. [PubMed: 16298994]
66. Amaya MF, Watts AG, Damager I, Wehenkel A, Nguyen T, Buschiazzi A, Paris G, Frasch AC, Withers SG, Alzari PM. *Structure* 2004;12:775–784. [PubMed: 15130470]
67. Murray BW, Wittmann V, Burkart MD, Hung SC, Wong CH. *Biochemistry* 1997;36:823–831. [PubMed: 9020780]
68. Poulin R, Lu L, Ackermann B, Bey P, Pegg AE. *J Biol Chem* 1992;267:150–158. [PubMed: 1730582]
69. Grishin NV, Osterman AL, Brooks HB, Phillips MA, Goldsmith EJ. *Biochemistry* 1999;38:15174–15184. [PubMed: 10563800]
70. McCann PP, Bacchi CJ, Clarkson AB Jr, Bey P, Sjoerdsma A, Schecter PJ, Walzer PD, Barlow JL. *The American journal of tropical medicine and hygiene* 1986;35:1153–6. [PubMed: 3098121]
71. Wallace HM, Fraser AV. *Amino Acids* 2004;26:353–365. [PubMed: 15290341]
72. Meyskens FL Jr, Gerner EW. *Clinical Cancer Research* 1999;5:945–951. [PubMed: 10353725]
73. van der Donk WA, Yu G, Perez L, Sanchez RJ, Stubbe J, Samano V, Robins MJ. *Biochemistry* 1998;37:6419–6426. [PubMed: 9572859]
74. Bhattacharjee MK, Snell EE. *J Biol Chem* 1990;265:6664–6668. [PubMed: 2182624]
75. Hayashi H, Tanase S, Snell EE. *Journal of Biological Chemistry* 1986;261:11003–9. [PubMed: 3733745]
76. Likos JJ, Ueno H, Feldhaus RW, Metzler DE. *Biochemistry* 1982;21:4377–4386. [PubMed: 6812624]
77. Ueno H, Likos JJ, Metzler DE. *Biochemistry* 1982;21:4387–4393. [PubMed: 6812625]
78. Thornberry NA, Bull HG, Taub D, Wilson KE, Gimenez-Gallego G, Rosegay A, Soderman DD, Patchett AA. *J Biol Chem* 1991;266:21657–21665. [PubMed: 1939194]
79. Thornberry NA, Bull HG, Taub D, Greenlee WJ, Patchett AA, Cordes EH. *J Am Chem Soc* 1987;109:7543–7544.
80. Xu Y, Abeles RH. *Biochemistry* 1993;32:806–811. [PubMed: 8422385]
81. Born TL, Myers JK, Widlanski TS, Rusnak F. *J Biol Chem* 1995;270:25651–25655. [PubMed: 7592741]
82. Myers JK, Cohen JD, Widlanski TS. *J Am Chem Soc* 1995;117:11049–11054.
83. Myers JK, Widlanski TS. *Science* 1993;262:1451–1453. [PubMed: 8248785]
84. Halazy S, Berges V, Ehrhard A, Danzin C. *Bioorg Chem* 1990;18:330–344.
85. Yaouancq L, Anissimova M, Badet-Denisot MA, Badet B. *Eur J Org Chem* 2002:3573–3579.
86. Araoz R, Anhalt E, Rene L, Badet-Denisot MA, Courvalin P, Badet B. *Biochemistry* 2000;39:15971–15979. [PubMed: 11123924]
87. Massiere F, Badet-Denisot MA, Rene L, Badet B. *J Am Chem Soc* 1997;119:5748–5749.
88. Luo Y, Knuckley B, Lee YH, Stallcup MR, Thompson PR. *J Am Chem Soc* 2006;128:1092–1093. [PubMed: 16433522]
89. Luo Y, Arita K, Bhatia M, Knuckley B, Lee YH, Stallcup MR, Sato M, Thompson PR. *Biochemistry* 2006;45:11727–11736. [PubMed: 17002273]
90. Berkowitz DB, Charette BD, Karukurichi KR, McFadden JM. *Tetrahedron: Asymmetry* 2006;17:869–882.
91. Capitani G, Tschoop M, Eliot AC, Kirsch JF, Gruetter MG. *FEBS Lett* 2005;579:2458–2462. [PubMed: 15848188]
92. Storici P, De Biase D, Bossa F, Bruno S, Mozzarelli A, Peneff C, Silverman RB, Schirmer T. *J Biol Chem* 2004;279:363–373. [PubMed: 14534310]
93. Silverman RB, Bichler KA, Leon AJ. *J Am Chem Soc* 1996;118:1241–1252.
94. Pedersen ML, Berkowitz DB. *J Org Chem* 1993;58:6966–6975.
95. Pedersen ML, Berkowitz DB. *Tetrahedron Lett* 1992;33:7315–7318.



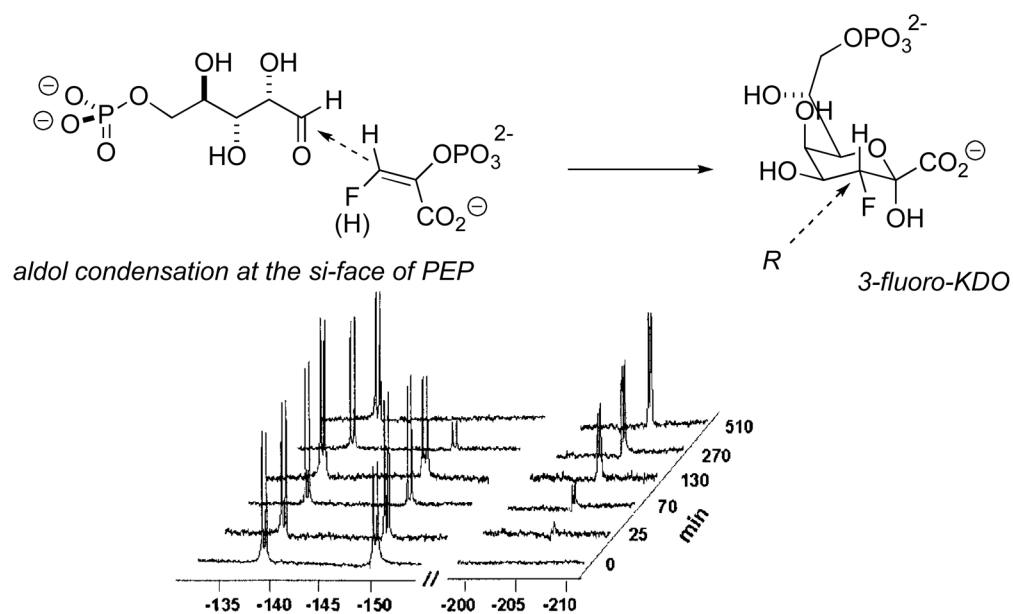
96. Berkowitz DB, Pumphrey JA, Shen Q. *Tetrahedron Lett* 1994;35:8743–8746.
97. Berkowitz DB, Smith MK. *Synthesis* 1996:39–41.
98. Berkowitz DB, McFadden JM, Chisowa E, Semerad CL. *J Am Chem Soc* 2000;122:11031–11032.
99. Seebach D, Fadel A. *Helv Chim Acta* 1985;68:1243–1250.
100. Naef R, Seebach D. *Liebigs Ann Chem* 1983:1930–1936.
101. Seebach D, Boes M, Naef R, Schweizer WB. *J Am Chem Soc* 1983;105:5390–5398.
102. Seebach D, Sting AR, Hoffmann M. *Angew Chem, Int Ed* 1997;35:2708–2748.
103. Berkowitz DB, Chisowa E, McFadden JM. *Tetrahedron* 2001;57:6329–6343.
104. Berkowitz DB, McFadden JM, Sloss MK. *J Org Chem* 2000;65:2907–2918. [PubMed: 10814177]
105. Comins DL, Salvador JM. *Journal of Organic Chemistry* 1993;58:4656–4661.
106. Berkowitz DB, Shen W, Maiti G. *Tetrahedron: Asymmetry* 2004;15:2845–2851.
107. Berkowitz DB, Maiti G. *Org Lett* 2004;6:2661–2664. [PubMed: 15281738]
108. Berkowitz DB, Bose M, Choi S. *Angew Chem Int Ed* 2002;41:1603–1607.
109. Berkowitz DB, Wu B, Li H. *Org Lett* 2006;8:971–974. [PubMed: 16494487]
110. Berkowitz DB, Pedersen ML. *J Org Chem* 1995;60:5368–9.
111. Berkowitz DB, Pedersen ML, Jahng WJ. *Tetrahedron Lett* 1996;37:4309–4312.
112. Berkowitz DB, De la Salud-Bea R, Jahng WJ. *Org Lett* 2004;6:1821–1824. [PubMed: 15151423]
113. McCarthy JR, Matthews DP, Stermerick DM, Huber EW, Bey P, Lippert BJ, Snyder RD, Sunkara PS. *J Am Chem Soc* 1991;113:7439–7440.
114. McCarthy JR, Matthews DP, Edwards ML, Stermerick DM, Jarvi ET. *Tetrahedron Lett* 1990;31:5449–5452.
115. Berkowitz DB, Jahng WJ, Pedersen ML. *Bioorg Med Chem Lett* 1996;6:2151–2156.
116. Leon AJ, Silverman RB. *Bioorg Med Chem Lett* 1996;6:1319–1322.
117. Silverman RB, Bichler KA, Leon AJ. *J Am Chem Soc* 1996;118:1253–1261.
118. Sukhareva BS, Dunathan HC, Braunshtein AE. *FEBS Letters* 1971;15:241–4. [PubMed: 11945855]
119. O’Leary MH, Baughn RL. *J Biol Chem* 1977;252:7168–7173. [PubMed: 561784]
120. O’Leary MH, Herreid RM. *Biochemistry* 1978;17:1010–1014. [PubMed: 629941]
121. Akhtar M, Stevenson DE, Gani D. *Biochemistry* 1990;29:7648–7660. [PubMed: 2271524]
122. Karukurichi KR, De la Salud-Bea R, Jahng WJ, Berkowitz DB. *J Am Chem Soc* 2007;129:258–259. [PubMed: 17212389]
123. Qu N, Ignatenko NA, Yamauchi P, Stringer DE, Levenson C, Shannon P, Perrin S, Gerner EW. *Biochemical Journal* 2003;375:465–470. [PubMed: 12859253]
124. Pan Y, Qiu J, Silverman RB. *J Med Chem* 2003;46:5292–5293. [PubMed: 14640537]

**Fig. 1.**

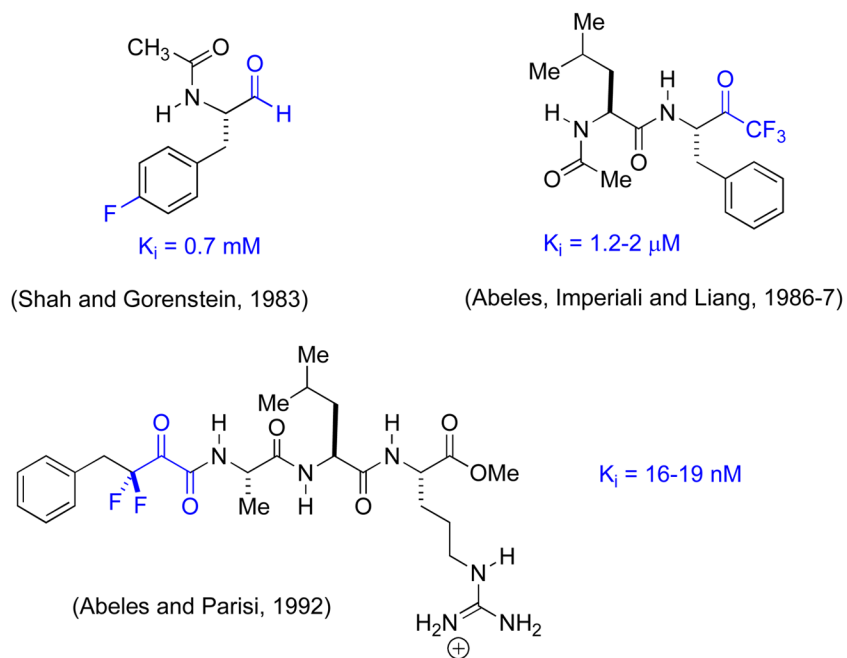
The 3-FABS method used to screen for protease and kinase activity simultaneously – pep = substrate peptide; P-pep = kinase product; C-pep = tryptic digestion product; <sup>19</sup>F NMR (564 MHz). (NMR figure adapted from ref 27)



**Fig. 2.** Polyfluorinated amino acids to improve sensitivity <sup>19</sup>F-NMR-based screening methods.

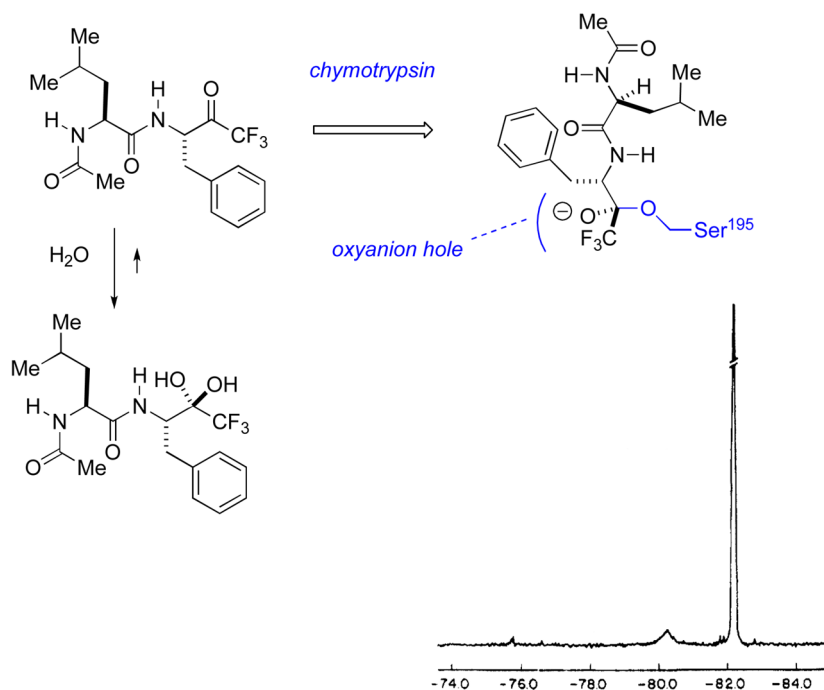
**Fig. 3.**

Use of a  $^{19}\text{F}$  stereochemical marker to decipher latent facial selectivity in the mechanism of KDO8P synthase ( $^{19}\text{F}$ NMR spectrum adapted from ref. 30)

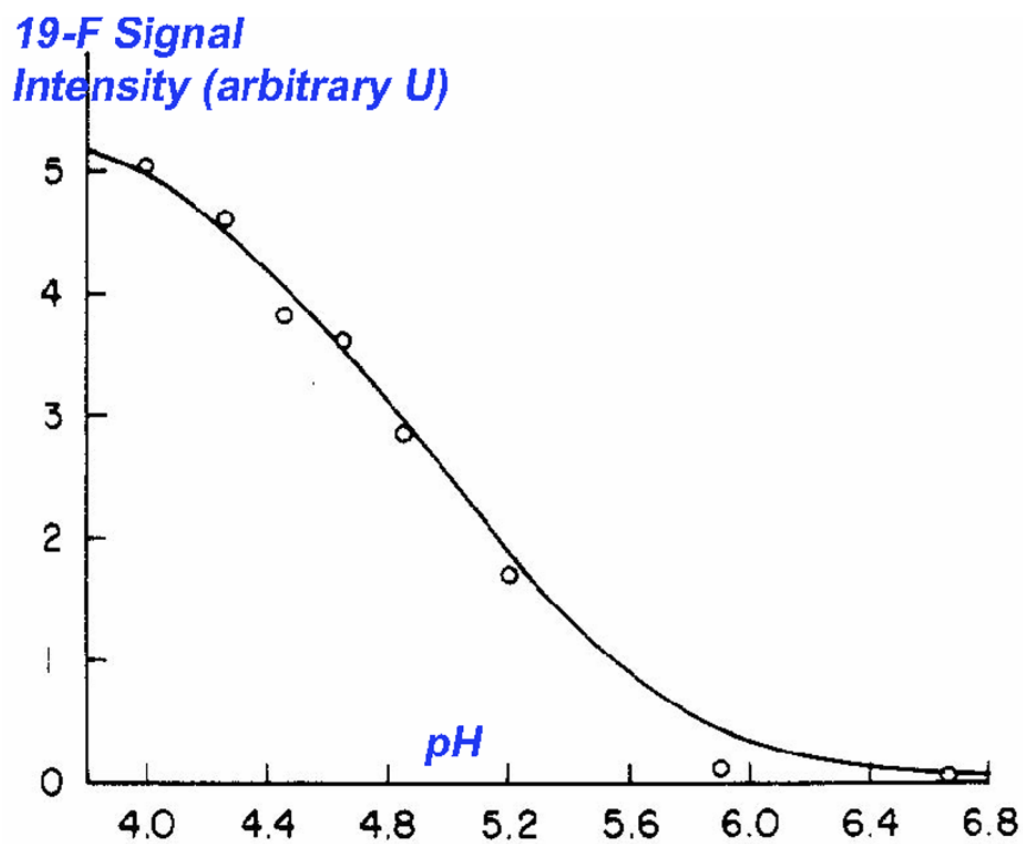


**Fig. 4.**  
Carbonyls with a high propensity for hydration serve as transition state analogue inhibitors for chymotrypsin.

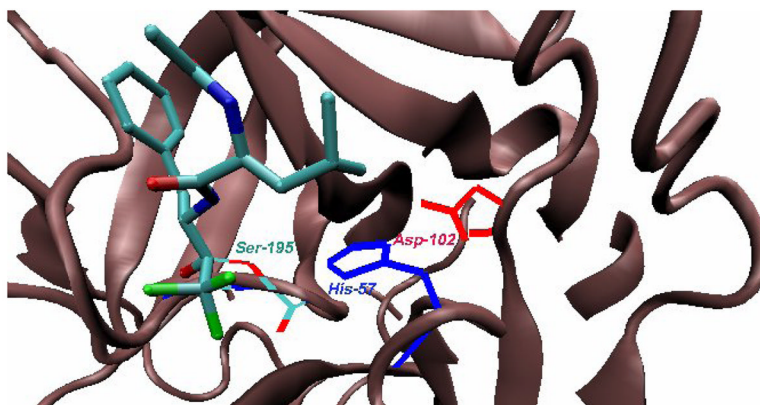




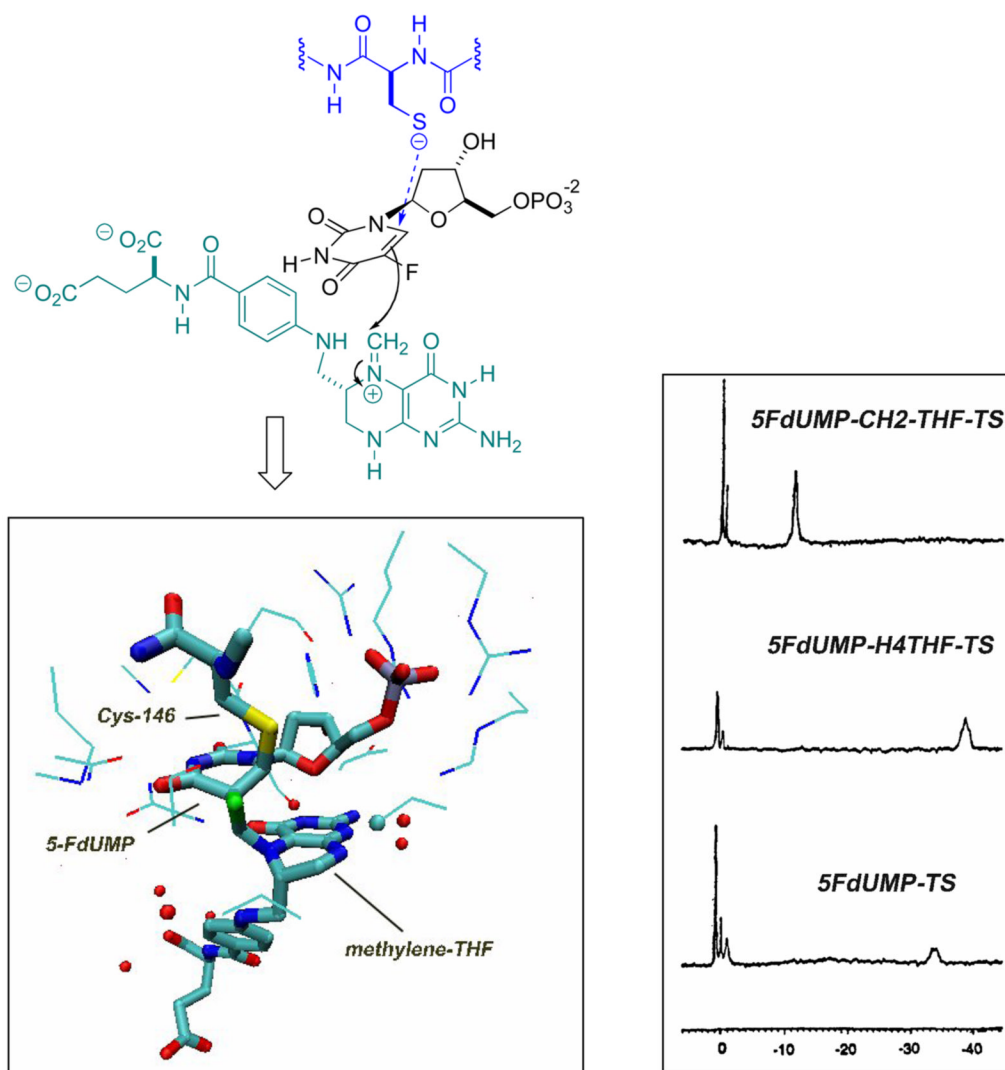
**Fig. 5.** Formation of the tetrahedral adduct with the active site serine of chymotrypsin. *Lower inset:* <sup>19</sup>F spectrum (adapted from ref. 31) showing both free inhibitor (hydrate, @ -82 ppm) and the covalent enzyme adduct (broad peak @ -80 ppm)



**Fig. 6.**  
 $^{19}\text{F}$  NMR titration of the TS-analogue complex shown in Figs. 5 and 7 (adapted from ref. 32)

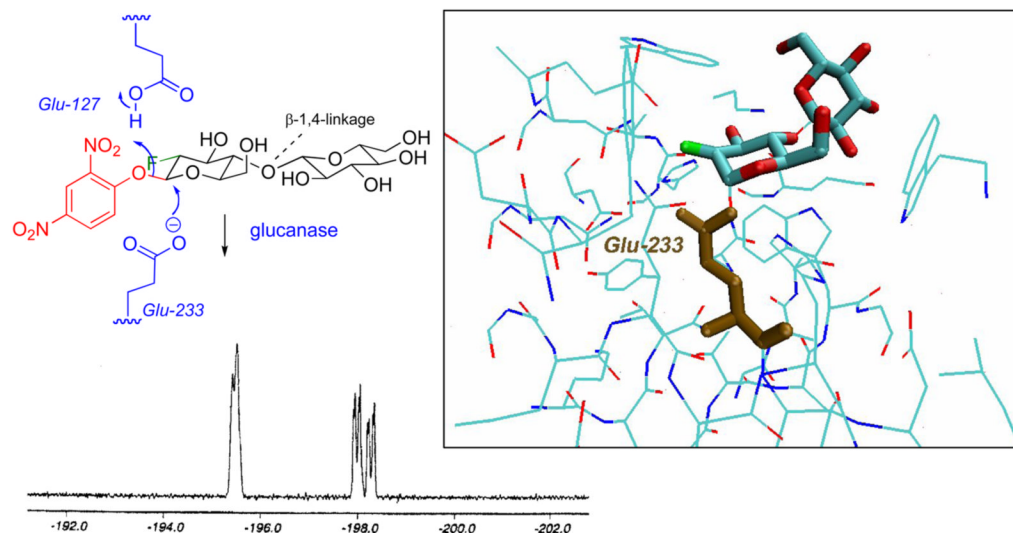


**Fig. 7.**  
X-Ray crystallographic view of the same transition state analogue complex shown in Fig. 5 (PDB ID 7GCH).



**Fig. 8.**

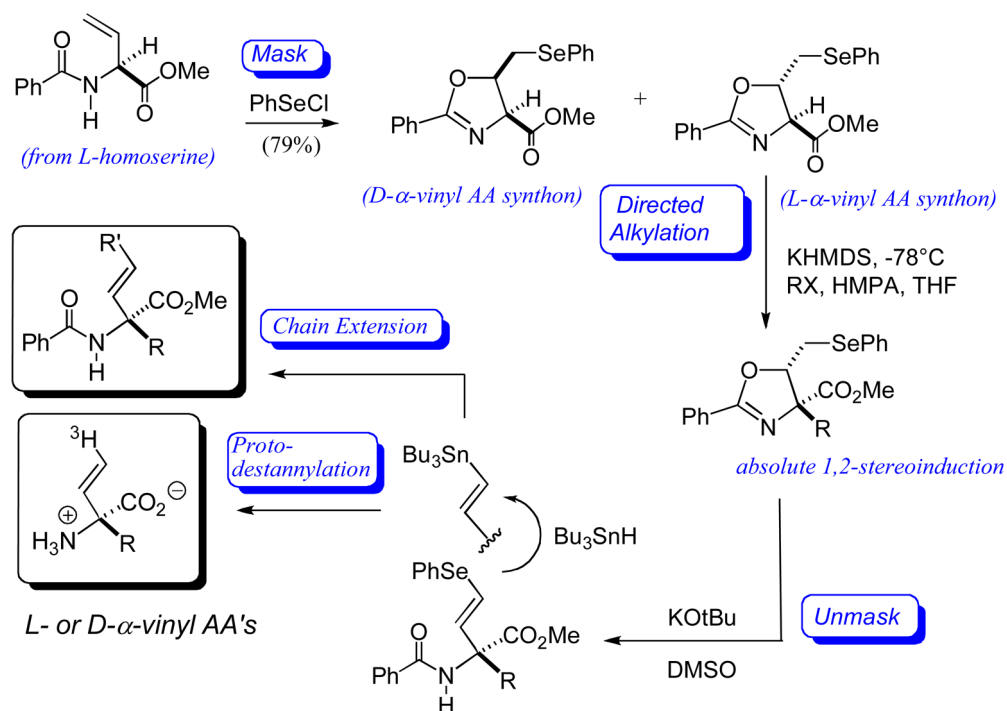
Formation of the 5F-dUMP-CH<sub>2</sub>-THF-TS ternary complex: *Top* - color-coded reaction scheme; *Bottom right* - 188.8 MHz <sup>19</sup>F NMR spectrum, showing progressive formation of the binary, pseudo-ternary and covalent ternary complex (adapted from ref 53); *Bottom left* - three-dimensional structure of the ternary complex (PDB ID:1TLS).



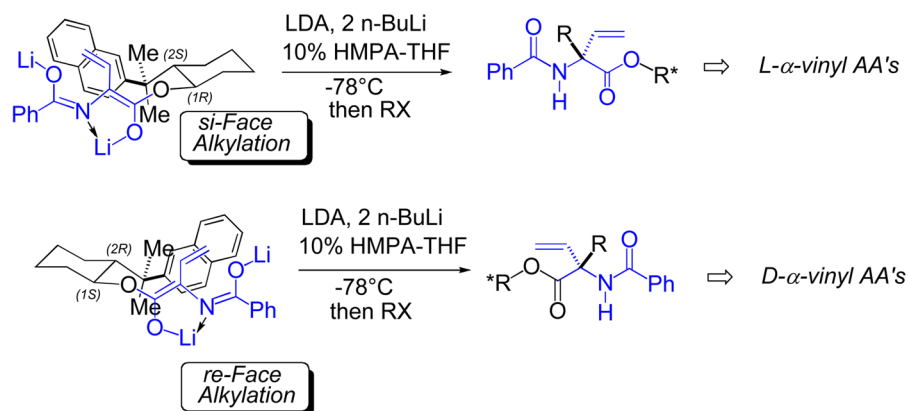
**Fig. 9.**

Use of the 2",4"-Dinitrophenyl 2-fluoro-2-deoxy-β-cellobioside to trap out the carboxylate residue in the active site of *Cellulomonas fimi* glucanase. *Lower Inset:* <sup>19</sup>F NMR of complex formation (adapted from ref. 58). The signals at -198.1 and -198.4 ppm are assigned to the unbound and hydrolyzed inhibitor, respectively. The broader signal at -195.4 ppm is due to the covalent intermediate. Note that the chemical shift (-205.5 ppm) of the adduct from the fluoro-sugar possessing the manno-stereochemistry unambiguously establishes the α-stereochemistry of the adduct with Glu-233. *Right hand inset:* View of the X-ray crystal structure of this complex (PDB ID: 1EXP).

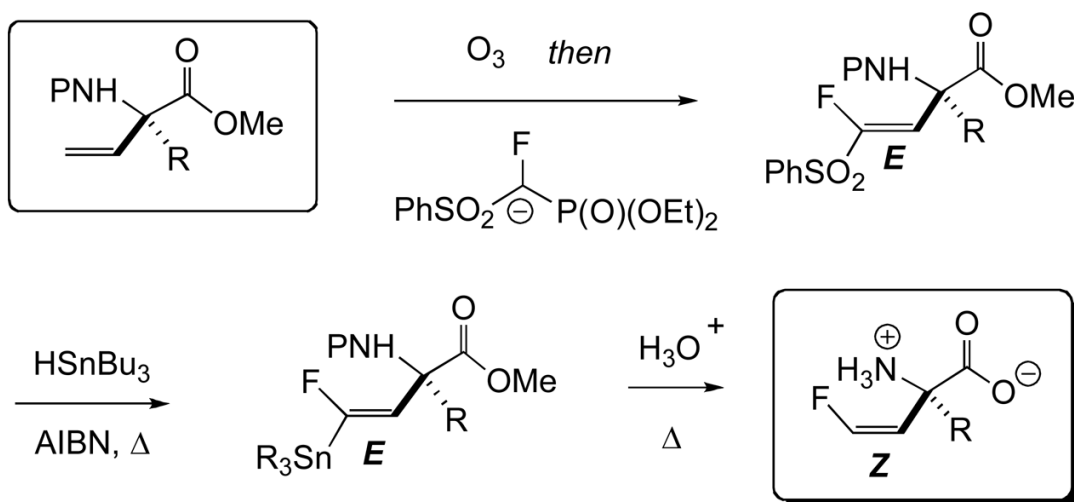


**Fig. 10.**

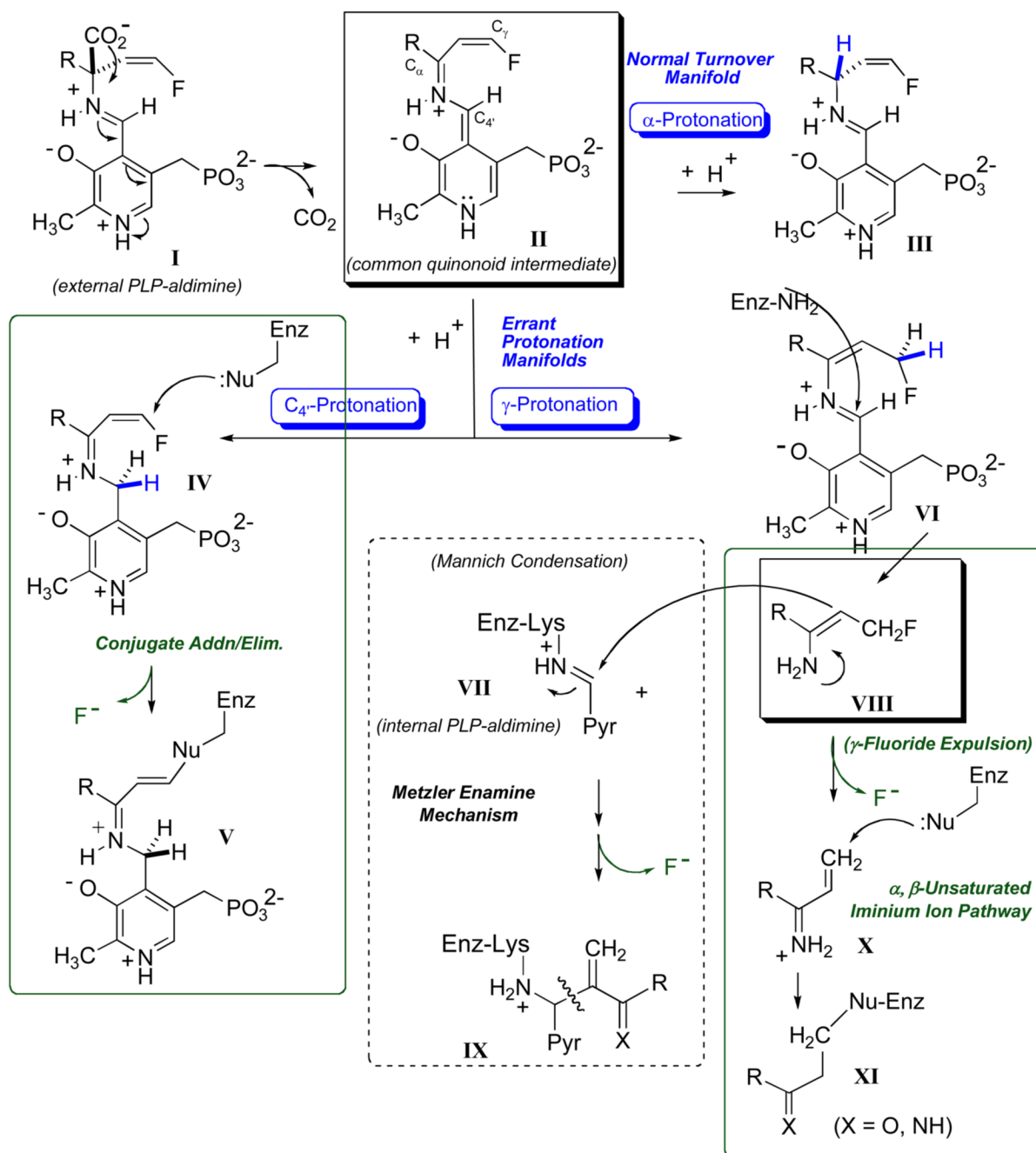
Asymmetric synthesis of quaternary,  $\alpha$ -vinyl amino acids via a "self-regeneration of stereocenters" approach.



**Fig. 11.** Asymmetric synthesis of quaternary,  $\alpha$ -vinyl amino acids via alkylation of chiral, vinylglycine-derived dienolates.



**Fig. 12.**  
Synthesis of quaternary,  $\alpha$ -(2'Z-fluoro)vinyl amino acids from the corresponding  $\alpha$ -vinyl amino acids.

**Fig. 13.**

Proposed mechanism of PLP-linked lysine decarboxylase inactivation with the new, quaternary,  $\alpha$ -(2'-fluoro)vinyl trigger. Green boxes highlight two projected electrophilic pathways for this functionality.

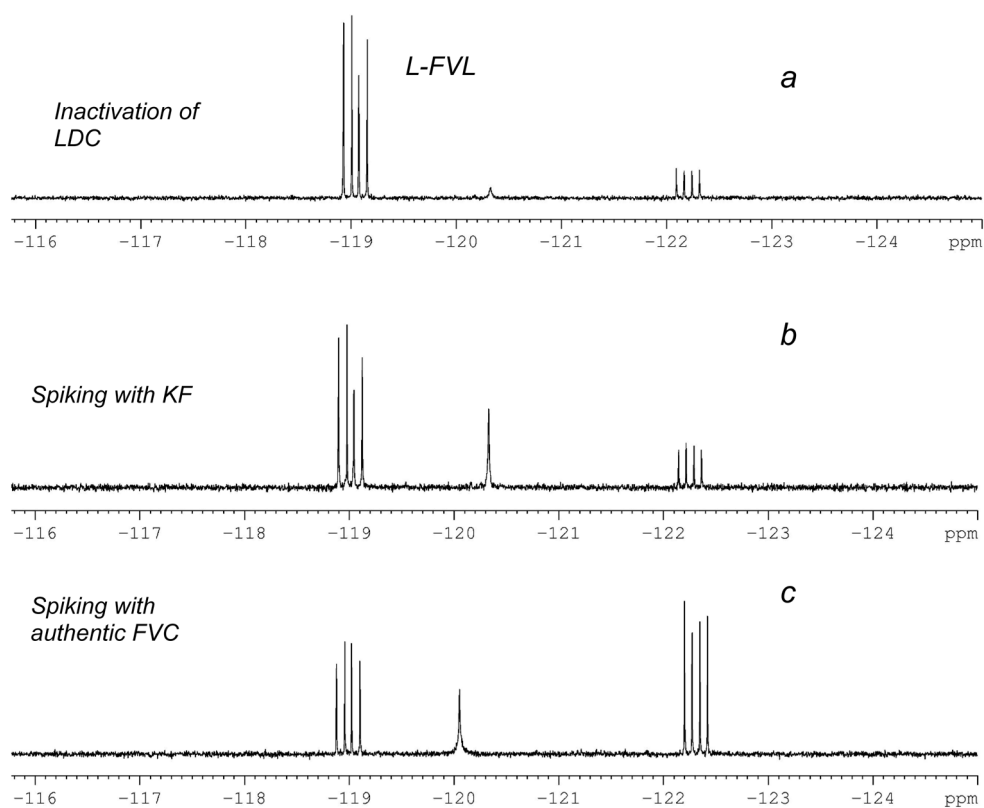


**Fig. 14.** Observation of turnover and aberrant protonation by 564 MHz  $^{19}\text{F}$  NMR (a)  $^{19}\text{F}$  NMR spectrum following inactivation of LDC with L- $\alpha$ -(2'-Z-fluoro)vinyllysine (L-FVL); (b) Addition of KF to (a); (c) Addition of  $\alpha$ -(2'-Z-fluoro)vinylcadaverine (FVC) to (b).